ChemComm

Accepted Manuscript

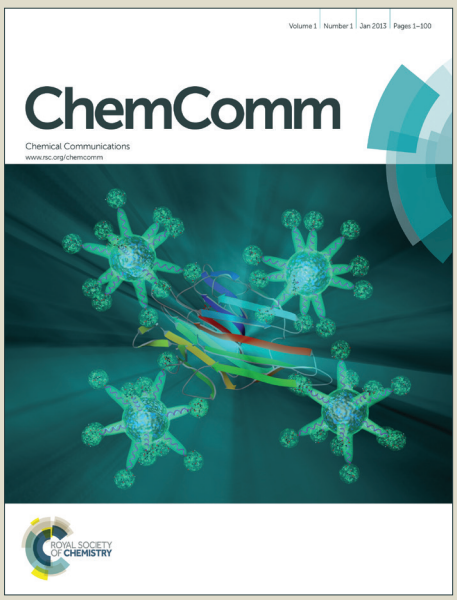

ROYAL SOCIETY OF CHEMISTRY

www.rsc.org/chemcomm

Journal Name

RSCPublishing

COMMUNICATION

Self-healing Catalysts: Co_3O_4 Nanorods for Fischer-Tropsch Synthesis

Cite this: DOI: 10.1039/x0xx00000x

Cun Wen,[a,b] Darrius Dunbar,[a] Xin Zhang,[c] Jochen Lauterbach,[a,b] Jason Hattrick-Simpers[a,b,*]

Received 00th January 2012,
Accepted 00th January 2012

DOI: 10.1039/x0xx00000x

www.rsc.org/

We combine kinetic and spectroscopic data to demonstrate the concept of a self-healing catalyst, which effectively eliminates the need for catalyst regeneration. The observed self-healing is triggered by controlling the crystallographic orientation at the catalyst surface.

Catalysts play a key role in reducing environmental pollution, and enabling future alternative energy solutions.[1, 2] A key problem for all catalytic processes is catalyst deactivation, which results in a decrease in production efficiency and increased maintenance costs.[3, 4] Normally, catalyst deactivation is addressed by optimizing the composition and particle size of the catalysts.[5] Although this may increase catalyst lifetimes, most catalysts still require periodic off-stream regeneration.[5, 6] It would be beneficial to prolong catalyst lifetimes by developing methods to render the catalyst self-healing while on-stream. For instance, one of the main deactivation mechanisms is the change of the catalyst oxidation state by oxidation or reduction (redox reactions).[7] In the context of catalyst deactivation by oxidation, a self-healing catalyst would be one that actively reduces the oxide as it grows. This approach would preserve the metallic state of the catalyst without separate steps for regeneration.

The goal for such an approach would be to design a highly reducible catalyst that preserves selectivity toward the preferred products but eliminates surface oxidation. This requires tuning the surface redox reaction to favor the reduction of the oxide to the metallic state. For instance, in Fischer-Tropsch synthesis (FTS), the primary reaction involves the hydrogenation of CO and polymerization of hydrocarbons. Water is produced in FTS as a side-product, up to 40 vol% in industrial reactors.[8-11] Metallic Co is the preferred catalyst for FTS [12 13], however, the presence of water has made it difficult to implement Co due to oxidation.[8-11] The oxidized Co is usually removed from the reaction stream and regenerated by hydrogen reduction.[14] Thus, tuning the redox reaction to favor reduction of the oxide *in-situ*, would preserve the metallic Co under reaction conditions and constitute a key advance in the field of FTS.

The nature of surface redox reactions can be altered by tuning the crystallographic facets exposed at catalyst surfaces.[15-18] For example, during electro-oxidation of formic acid and ethanol, Pt nanocrystals with high-index {730} surface facets, which contain low coordination number atoms, are more active than low-index, {111} faceted Pt nanospheres.[15] Similarly, water oxidation is more readily catalysed by the (040) surface of $BiVO_4$ than by (110) surfaces.[19] Another recent report illustrated significant enhancement of surface redox reactions on cobalt oxide nanorods, as compared with cobalt oxide nanoparticles.[20] Cobalt oxide nanorods exhibit {110} facets with both Co^{2+} and Co^{3+} exposed on the surface. In contrast, the nanoparticles possess {111} and {001} facets where the only surface species is Co^{2+}.[20] A similar effect of faceting has been observed for the electrocatalytic oxygen reduction in cobalt oxide nanocatalysts for DMFC.[21] This effect suggests that by carefully selecting the crystallographic planes of Co_3O_4 exposed at the catalyst surface, the reduction of the catalyst could be promoted, effectively negating oxidation during FTS.[22-26]

Although the aforementioned studies have demonstrated that redox reactions can be tuned by catalyst faceting, the role of this faceting on preserving the catalyst's metallic state has not been explored.[8] Here, we demonstrate the first study of a self-healing catalyst obtained by controlling catalyst crystal faceting using Co nanoparticles and nanorods as proof-of-principle. The origin of the resistance to water oxidation during FTS is illustrated via reactor studies, XPS, and *in-situ* Raman spectroscopy.

The Co nanorods and nanoparticles studied were synthesized following literature,[20, 27] and the general morphologies are shown in the transmission electron microscopy (TEM) images, Fig. 1 and Figs. S1a and S1b. The diameter of the Co nanorods is in the range of 10-20 nm, and their length is typically within 200-300 nm, which is consistent with literature.[20, 27] The synthesized Co nanoparticles exhibit particle sizes between 10 nm and 40 nm. The particle sizes of the nanorods and nanoparticles are comparable to the size range (10-210 nm) typically investigated for model FTS catalysts.[28-30] In this range, the turnover frequency of the Co catalyst does not change with particle size.[31] Both the as-synthesized Co nanorods and the nanoparticles have the Co_3O_4 spinel structure (PDF 41-1467), as

determined by powder X-ray diffraction, see insets in Fig. S1a and S1b.

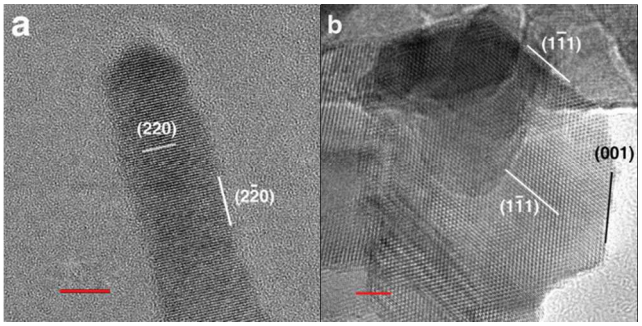

Fig. 1 HRTEM images of a) nanorods and b) nanoparticles, (scale bar corresponds to 5 nm), and c) models of {110} and {001} facets.

The crystal facets exposed on the nanorod and nanoparticle surfaces were characterized with high resolution TEM, see Figs 1a and b. The *d*-spacing (2.83 ± 0.03Å) measured by HRTEM on the Co_3O_4 nanorods is consistent with the (220) of Co_3O_4 and results in the exposure of the {110} family of facets at their surface.[20] In contrast, the Co nanoparticles exhibit {001} and {111} facets at their surfaces (Fig. 1b), which is consistent with literature.[20] As stated above this corresponds to distinct distributions of cations being presented at the surfaces of nanorods and nanoparticles. [20, 27] The presence of the different oxidation states of Co on the surface results in substantial differences in the reduction temperature of the respective nanostructures. Temperature programmed reduction Raman spectroscopy (Raman TPR) experiments, Fig. S2, demonstrate that the nanorods are reduced to Co^0 by 533 K, which is approximately 60 K lower than the reduction temperature for the nanoparticles (593 K). The lower reduction temperature of Co^{3+} is commensurate with the typical reaction conditions for FTS (473-573 K).[14, 22] This suggests an ability to reverse oxidation of the catalyst during operation. After reduction at 773 K under hydrogen, the Co_3O_4 nanoparticles and nanorods were reduced to metallic Co, as indicated by XPS measurements (see Fig. S3). The binding energy of Co $2p_{3/2}$ on both Co nanoparticles and nanorods is 777.9 ±0.3 eV in the XPS profiles, consistent with metallic cobalt (778.2 ev).[32]

Following reduction, the FTS activity and selectivity of Co nanoparticles and nanorods were measured at 543 K before and during the addition of water (25 vol. %) to the reactant feed. On the nanoparticles, once water was introduced into the feed, the activity and selectivity changed substantially. The conversion of CO increased from 5 ± 1% to 13 ± 3%, the selectivity towards CO_2 increased from about 14 ± 2% to 65 ± 4%, and the selectivity towards C_{5+} hydrocarbons decreased from 31 ± 2% to 15 ± 2%, (Fig.. 2a) in accordance with literature.[9-11] The changes in CO_2 and C_{5+} selectivity and the CO conversion can be attributed to the oxidation of surface Co^0. This decreases the activity toward long-chain hydrocarbons, but promotes the water-gas-shift (WGS) reaction to produce CO_2.[33]

The nanorods exhibited CO conversion in excess of 92 ±4%, at comparable conditions to the nanoparticles (Fig. S4a). No significant change of the FTS behavior was observed for the nanorods after 10 hours on stream in water-rich conditions. The high conversion (> 15%) may lead to mass and heat transfer limitations.[34] Therefore, the reaction temperature and gas hourly space velocity were varied separately to reduce conversion (Fig. 2b and Fig. S4). For instance, the temperature was lowered from 543 K to 433 K to reduce the CO conversion to 12% ± 2%, the C_{5+} selectivity was lowered to 3% ± 1% and the CO_2 selectivity was found to be 40%± 3%. A table summarizing the results can be found in the supporting information. During reactions for all conditions no change in conversion or selectivity was observed after more than 10 hours of exposure to the water rich reaction conditions, see Fig. 2b. The nanorods were tested at a reaction temperature 100 K below their Raman TPR measured reduction temperature, and still did not exhibit any changes to their catalytic activity during water-enriched FTS. Experiments were also conducted over a 20 h period without any degradation in FTS performance.

To elucidate the mechanism of the observed resistance to

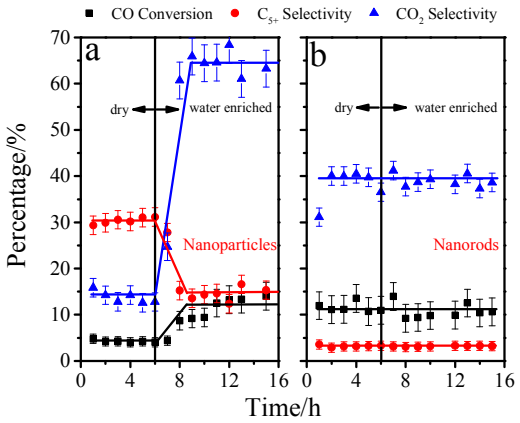

Fig. 2 Fischer-Tropsch synthesis on a) nanoparticles and b) nanorods at low CO conversion. At 6 hours, 25 vol. % of water were added to the feed stream. The dashed lines were added as a guide to the eyes.

oxidation, *in situ* Raman spectra were taken on both nanorods and nanoparticles. Prior to catalyst activation by hydrogen reduction, both nanorods and nanoparticles exhibited Raman spectra corresponding to Co_3O_4, as shown in Fig. S2.[35] After reduction at 773 K, *in situ* Raman spectra were taken to characterize the phase of the catalyst surface during reactions under FTS conditions and water-rich FTS conditions. As shown in Fig. 3a, dosing the nanoparticles with water-rich syngas at 543 K results in the appearance of a peak located at 591 cm^{-1}, corresponding to CoOOH an intermediate for the formation of Co_3O_4.[36, 37] The intensity of this peak, which is correlated to the amount of CoOOH present on the catalyst, increases steadily with time. This result is consistent with previous observations showing that Co nanoparticles are oxidized by water during FTS, resulting in the observed change in FTS activity shown in Fig. 2a.[38, 39]

For the Co nanorods, in contrast, *in situ* Raman shows (Fig. 3b) that the formation of CoOOH is limited and reversible at 543 K. In conjunction with the FTS reaction data, the Raman results indicate that the nanorod-based catalyst self-heals during water dosing by reducing the oxide as it is formed.

The mechanism behind the observed difference in the oxidation of the two morphologies can be understood by examining the difference in the reduction potential of the two oxidation states of Co presented at their surfaces. On nanoparticles, only Co^{2+} sites, with a reduction potential to the metallic state of -0.28 V (referring to standard hydrogen electrode set as 0 V), will be present at the outermost surface according to the HRTEM images (Fig.. 1b). [40] This corresponds to a positive (54 kJ mol^{-1}) Gibbs free energy for hydrogen reduction from Co^{2+} to Co^0, indicating that the reaction is unfavorable.[41] Contrarily, on the Co nanorods, Co^{3+} is present on the surface due to the preferential exposing of {110} facets (shown in Fig.. 1a), and the Gibbs free energy of reduction to Co metal is -122 kJ mol^{-1} (0.42 V).[40] Thus, the reversibility of oxidation on the Co

nanorods as observed by *in situ* Raman spectra, and subsequent insensitivity of activity and selectivity on the nanorods to water dosing, can be attributed to the reduction potential of the Co^{3+} species.

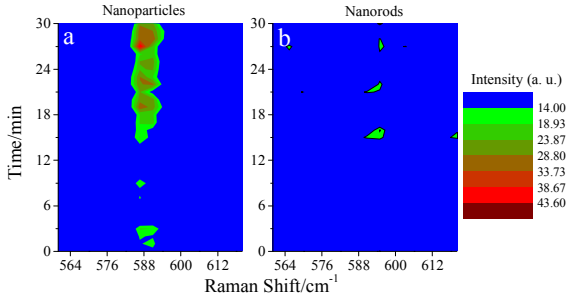

Fig. 3 *in situ* Raman spectra of nanoparticles and nanorods during water enriched FTS reactions. The nanorods are seen to reverse formation of CoOH.

Conclusions

In summary, we have demonstrated the concept of novel self-healing catalysts that eliminate the need for periodic regeneration. The self-healing functionality is accomplished by tuning the crystallographic facets exposed on the active catalyst surface. The observed phenomenon is proposed to result from the exposure of {110} surfaces on the nanorods, which present the readily reducible Co^{3+} on the surface. The Co^{3} cation promotes reduction of the water oxidized catalyst. The concept of a self-healing catalyst represents an avenue towards extending catalyst lifetimes in many catalytic reactions during which water can oxidize and deactivate the catalysts. For instance, during hydrodeoxygenation of 4-methylphenol on NiMo catalysts, water can oxidize the Ni to nickel oxide and result in a loss of catalytic activity. The results from this work, however, indicate a possible strategy for imparting self-healing properties to the metallic catalyst by using faceting to preferentially expose more readily reducible cations.

The work is supported by the South Carolina Center of Economic Excellence for Strategic Approaches to the Generation of Electricity and ORAU under the Ralph E. Powe Junior Faculty Enhancement Award. We acknowledge the support from Dr. Briber, and the Maryland NanoCenter and NispLab. The NispLab is supported in part by the NSF as a MRSEC Shared Experimental Facility.

Notes and references

[a] Department of Chemical Engineering, University of South Carolina, Columbia, SC, 29201
[b] Center of Economic Excellence for Strategic Approaches to the Generation of Electricity, University of South Carolina, Columbia, SC, 29201
[c] Department of Materials Science and Engineering, University of Maryland, 9314 Cherry Hill Road #1020, College Park, MD, 20740

† Electronic Supplementary Information (ESI) available: Detailed experimental procedures, The TEM images of Co_3O_4 nanoparticles and nanorods (Fig.. S1), the in situ Raman spectra (Fig.. S2), the X-ray photoelectron spectra of Co nanoparticles and nanorods after reduction at 773K (Fig.. S3), the FTS performance on nanorods at different space velocity (Fig.. S4), and a table of conversion and selectivity for the different experiments (Table S1). See DOI: 10.1039/c000000x/

1. A. T. Bell, *Science*, 2003, **299**, 1688-1691.
2. M. Boudart, B. H. Davis and H. Heinemann, *Introduction*, Wiley-VCH Verlag GmbH, 2008.
3. L. A. Vytnova, G. A. Kliger, E. I. Bogolepova, V. I. Kurkin, A. N. Shuikin, M. P. Filatova, E. V. Marchevskaya and E. V. Slivinskii, *Petrol Chem+*, 2003, **43**, 74-80.
4. J. J. Spivey, G. W. Roberts and B. H. Davis, *Catalyst deactivation*, Elsevier, Amsterdam, the Netherlands, 2001.
5. P. Forzatti and L. Lietti, *Catal Today*, 1999, **52**, 165-181.
6. J.-S. Choi, W. P. Partridge and C. S. Daw, *Applied Catalysis A: General*, 2005, **293**, 24-40.
7. P. G. Menon, *Chem Rev*, 1994, **94**, 1021-1046.
8. D. Baudouin, K. C. Szeto, P. Laurent, A. De Mallmann, B. Fenet, L. Veyre, U. Rodemerck, C. Copéret and C. Thieuleux, *J Am Chem Soc*, 2012, **134**, 20624-20627.
9. M. Lualdi, S. Lögdberg, G. Di Carlo, S. Järås, M. Boutonnet, A. Venezia, E. Blekkan and A. Holmen, *Top Catal*, 2011, **54**, 1-10.
10. E. van Steen, M. Claeys, M. E. Dry, J. van de Loosdrecht, E. L. Viljoen and J. L. Visagie, *The Journal of Physical Chemistry B*, 2005, **109**, 3575-3577.
11. E. Iglesia, S. L. Soled, R. A. Fiato and G. H. Via, *J Catal*, 1993, **143**, 345-368.
12. J. Cheng, P. Hu, P. Ellis, S. French, G. Kelly and C. M. Lok, *The Journal of Physical Chemistry C*, 2009, **114**, 1085-1093.
13. T. Patzek and G. Croft, *Natural Resources Research*, 2009, **18**, 181-191.
14. M. E. Dry, in *Studies in Surface Science and Catalysis*, eds. S. André and D. Mark, Elsevier, 2004, pp. 533-600.
15. N. Tian, Z.-Y. Zhou, S.-G. Sun, Y. Ding and Z. L. Wang, *Science*, 2007, **316**, 732-735.
16. D. Wang, H. Jiang, X. Zong, Q. Xu, Y. Ma, G. Li and C. Li, *Chemistry – A European Journal*, 2011, **17**, 1275-1282.
17. R. Si and M. Flytzani-Stephanopoulos, *Angewandte Chemie International Edition*, 2008, **47**, 2884-2887.
18. G. Liu, J. C. Yu, G. Q. Lu and H.-M. Cheng, *Chem Commun*, 2011, **47**, 6763-6783.
19. S. B. Rasmussen, S. Perez-Ferreras, M. A. Bañares, P. Bazin and M. Daturi, *ACS Catalysis*, 2012, 86-94.
20. X. W. Xie, Y. Li, Z. Q. Liu, M. Haruta and W. J. Shen, *Nature*, 2009, **458**, 746-749.
21. J. Xu, P. Gao and T. S. Zhao, *Energ Environ Sci*, 2012, **5**, 5333-5339.
22. B. de Rivas, R. López-Fonseca, C. Jiménez-González and J. I. Gutiérrez-Ortiz, *Chem Eng J*, 2012, **184**, 184-192.
23. L. Hu, Q. Peng and Y. Li, *J Am Chem Soc*, 2008, **130**, 16136-16137.
24. L. Yan, X. Zhang, T. Ren, H. Zhang, X. Wang and J. Suo, *Chem Commun*, 2002, 860-861.
25. Y. Liang, Y. Li, H. Wang, J. Zhou, J. Wang, T. Regier and H. Dai, *Nat Mater*, 2011, **10**, 780-786.
26. C.-J. Jia, M. Schwickardi, C. Weidenthaler, W. Schmidt, S. Korhonen, B. M. Weckhuysen and F. Schüth, *J Am Chem Soc*, 2011, **133**, 11279-11288.
27. X. Xie, P. Shang, Z. Liu, Y. Lv, Y. Li and W. Shen, *The Journal of Physical Chemistry C*, 2010, **114**, 2116-2123.
28. E. Iglesia, S. L. Soled and R. A. Fiato, *J Catal*, 1992, **137**, 212-224.
29. G. L. Bezemer, J. H. Bitter, H. P. C. E. Kuipers, H. Oosterbeek, J. E. Holewijn, X. Xu, F. Kapteijn, A. J. van Dillen and K. P. de Jong, *J Am Chem Soc*, 2006, **128**, 3956-3964.
30. E. Iglesia, *Applied Catalysis A: General*, 1997, **161**, 59-78.
31. J. P. den Breejen, P. B. Radstake, G. L. Bezemer, J. H. Bitter, V. Froseth, A. Holmen and K. P. de Jong, *J Am Chem Soc*, 2009, **131**, 7197-7203.
32. C. R. Brundle, T. J. Chuang and D. W. Rice, *Surf Sci*, 1976, **60**, 286-300.
33. J. R. Mellor, R. G. Copperthwaite and N. J. Coville, *Applied Catalysis A: General*, 1997, **164**, 69-79.
34. R. J. H. Voorhoeve and J. C. M. Stuiver, *J. Catal.*, 1971, **23**, 228-235.
35. V. G. Hadjiev, M. N. Iliev and I. V. Vergilov, *Journal of Physics C: Solid State Physics*, 1988, **21**, L199-L201.
36. C.-W. Tang, C.-B. Wang and S.-H. Chien, *Thermochim Acta*, 2008, **473**, 68-73.
37. T. Pauporté, L. Mendoza, M. Cassir, M. C. Bernard and J. Chivot, *J. Electrochem. Soc.*, 2005, **152**, C49-C53.
38. G. P. Huffman, N. Shah, J. M. Zhao, F. E. Huggins, T. E. Hoost, S. Halvorsen and J. G. Goodwin, *J Catal*, 1995, **151**, 17-25.
39. A. M. Hilmen, D. Schanke, K. F. Hanssen and A. Holmen, *Applied Catalysis A: General*, 1999, **186**, 169-188.
40. W. M. Haynes, *CRC Handbook of Chemistry and Physics*, 2011.
41. I. Levine, *Physical Chemistry*, McGraw-Hill, 2008.